Improved Control Strategy for Fuel Cell and Photovoltaic Inverters in a Microgrid

A A SALAM, A MOHAMED, M A HANNAN
Department of Electrical, Electronic and Systems Engineering
Universiti Kebangsaan Malaysia,
Bangi, Selangor 43600 MALAYSIA
azuki@eng.ukm.my, azah@eng.ukm.my

Abstract: - This paper presents an improved control strategy for parallel inverters so as to better manage power sharing among the distributed generation units in a microgrid. The proposed control strategy combines both power and voltage control schemes implemented on the voltage source inverters which are used as power electronics interface systems for conversion of power generated by fuel cell and photovoltaic generation units. Dynamic models of the fuel cell and photovoltaic systems available in the PSCAD/EMTDC simulation software are used as distributed generation units present in the microgrid. To evaluate the effectiveness of the developed control strategy, the microgrid is operated in grid connected, islanding and transition modes of operation.

Key-Words: - Distributed generation, microgrid, fuel cell, photovoltaic, inverter

1 Introduction

A cluster of distributed generation (DG) units are usually connected to a distribution network to maintain the reliability of critical loads, especially when the grid supply is not available. However, an increase in the number of DG connections can give rise to several technical concerns in the operation of the power system. To overcome this problem, a microgrid is formed when multiple DG units in electrical proximity to each other are grouped together in a distribution system. Thus, the microgrid concept assumes a cluster of loads and DG units operating as a single controllable system that provides both power and heat to its local area [1]. From the grid's point of view, a microgrid can be regarded as a controlled entity within a power system that can be operated as a single aggregated load and as a small source of power supporting the network. From a customer point of view, microgrids are considered to provide their thermal and electricity needs, enhance local reliability, reduce emissions, improve power quality by supporting voltage and reducing voltage sags and potentially reduce costs of energy supply.

The DG units in a microgrid may take many forms of technologies, namely, diesel engines, micro turbines, fuel cells, photovoltaics and wind turbines. The capacity of the DG units usually varies from few kWs to 1-2 MWs. The form of the microgrid takes with the different types of DG units and loads will have a large impact on the operating and control regime of the system. Therefore, coordinated operation and control of DG units together with storage devices, such as flywheels, energy capacitors, batteries, and controllable loads are central to the concept of microgrids.

The control strategies in DG units are selected based on the required functions and possible operation scenarios. They are also determined by the nature of their interactions with the system and the other DG units. A study about islanding detection of the system with a single DG unit is performed to examine the impacts of controls in islanding detection and non-detection zone [2]. However, it did not cover the impacts of the control technique in grid-connected and stand-alone mode. Ref. [3] utilizes the current and voltage control techniques for voltage source inverters to stabilize load voltage. The method is able to perform well in both stand-alone operation and grid-connected mode. In stand-alone operation the method optimizes the power performance of the system. A new voltage control strategy for inverter-based DG units is proposed in [4]. It shows smooth transition from grid-connected to islanded modes, besides from its ability to perform in different mode of operations mentioned before. However, the disadvantage of the approach is the lack of maximum power delivery from the DG units.

A microgrid with multiple DG units must have the capability to operate either in grid connected mode or in islanding mode depending on factors like planned disconnection, grid outages or economical convenience [5,6]. Considering the operating modes, a series of technical challenges with regards to the operation and control of microgrids need to be addressed such as sharing of loads between DG units and smooth switching from grid-connected to island operation. An important consideration in managing microgrids is to control the parallel operation of inverters so that they can work efficiently to achieve high performance. In [7], a master/slave control scheme for operating the DG units both in grid-connected and islanding modes was developed. Here, two local controls schemes for master/slave operation were used. However, a drawback of this control method is that there is a need for having one unit to act as a master unit and if this unit fails the overall system will be down.

A phase-locked loop control technique is commonly used in grid-connected converters to provide accurate estimation of phase angle for grid synchronization [8]. Another control scheme known as the voltage and frequency droop control method is proposed to obtain good sharing of the parallel inverters for different modes of operation [9]. The droop control method makes the parallel inverters share both active and reactive powers, which allows power management on power lines for far-away parallel inverters. This approach does not directly incorporate the load dynamics in the control loop, large or fast load changes and hence may result in either poor dynamic response or even voltage/frequency instability. Thus, it is very important for the microgrid to utilize the local measurements of the parallel inverters to achieve better active and reactive power sharing.

In this paper, an improved control strategy is presented, which is able to better manage power sharing accuracy of the parallel connected inverters used in a microgrid. The developed control strategy combines the advantages of both power and voltage control schemes. Power control ensures stability of the whole conversion system, while voltage control allows a more accurate generation of the reference voltage necessary to apply in the pulse width modulation technique. The combined use of power and voltage control schemes allow the implementation of a simple and effective three-phase control scheme, particularly to deal with critical conditions that can occur in the microgrids. To test the performance of the proposed control strategy, simulations were carried out by considering two DG units, namely fuel cell and photovoltaic connected to the grid system.

2 Microgrid System Configuration

The microgrid system consisting of two DG units, a radial distribution system, six transformers with voltage levels of 132/11 kV and 11/0.415 kV and three loads with a 100 kW capacity for each load is shown in Figure 1. The DG units and loads are operated at 0.415 kV and connected to the distribution grid through the transformers, lines and a switch. The DG units comprise of solid oxide fuel cell (SOFC) and photovoltaic arrays which are connected to the grid through converters. The two DG units are controlled such that they can provide local power and voltage support for loads 1 to 3. This configuration reduces the burden on generation and ensures the delivery of power directly from the main grid. It also enhances the immunity of critical loads to system disturbances in the grid.

The distributed generation powered by fuel cell and photovoltaic has gained popularity due to their higher operating efficiency, improved reliability and lower emissions. Fuel cell is attractive because it is modular, efficient and environmentally friendly. The dynamic models of SOFC and photovoltaic are described accordingly.

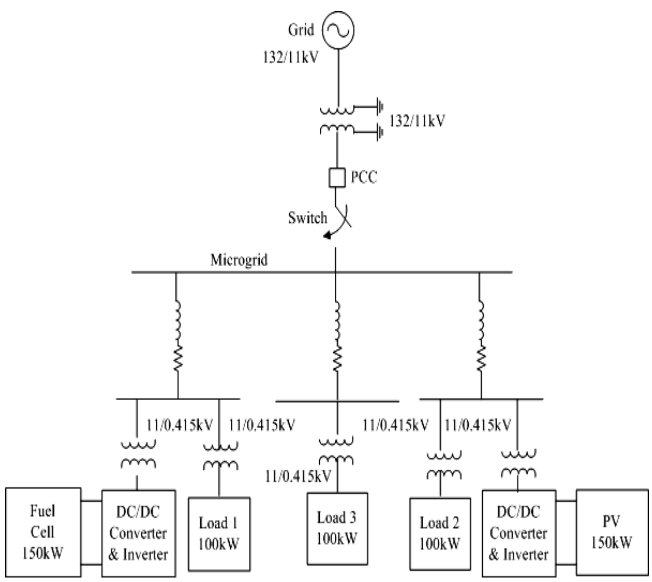

Fig.1 Microgrid System Configuration

2.1 Solid oxide fuel cell model

The SOFC model is derived by considering the total stack voltage of the fuel cell stack [10]. Considering ohmic losses of the stack, the expression of total stack voltage can be written as,

$$V_{fc} = N_0\left(E_0 + \frac{RT}{2F}\left(\ln\frac{P_{H_2}P_{O_2}^{\,0.5}}{P_{H_2O}}\right)\right) - rI_{fc} \qquad (1)$$

where,

V	: Total stack voltage
E_0	: Standard reversible cell potential
r	: Internal resistance of stack
I	: Stack current
N	: Number of cells in stack
R	: Universal gas constant
T	: Stack temperature
F	: Faraday's constant
PH_2	: Partial pressure of hydrogen
PO_2	: Partial pressure of oxygen
PH_2O	: Partial pressure of water

The output voltage of the stack is given by the Nernst equation. The ohmic loss of the stack is due to the resistance of the electrodes and the resistance of the flow of oxygen ions through the electrolyte. Partial pressure of hydrogen, oxygen and water are given in Equations (2), (3) and (4). The slow dynamics of the fuel cell current is represented by Equation (5).

$$P_{H_2} = \left(\frac{\frac{1}{KH_2}}{1+\tau_{H_2}S}\right)(qH_2 - 2K_rI) \qquad (2)$$

$$P_{O_2} = \left(\frac{\frac{1}{KO_2}}{1+\tau_{O_2}S}\right)(qO_2 - 2K_rI). \qquad (3)$$

$$P_{H_2O} = \left(\frac{\frac{1}{KH_2O}}{1+\tau_{H_2}OS}\right)(2K_rI) \qquad (4)$$

$$I = \left(\frac{I_{ref}}{1+\tau_e S}\right) \qquad (5)$$

I_{ref} is the reference current which is given by Equation (6). Fuel and oxygen flow are given by Equations (7) and (8).

$$I_{ref} = \left(\frac{P_{ref}}{V_{fc}}\right) \qquad (6)$$

$$qH_2^r = 2K_rI \qquad (7)$$

$$qO_2^r = \frac{qH_2}{rHO} \qquad (8)$$

The total power generated by the fuel cell is given by,

$$P_{fc} = N_oVI \qquad (9)$$

Figure 2 shows the PSCAD/EMTDC simulation model of the fuel cell system based on the mathematical model of the SOFC. The parameters of the SOFC are obtained from [11] and shown as in Table 1.

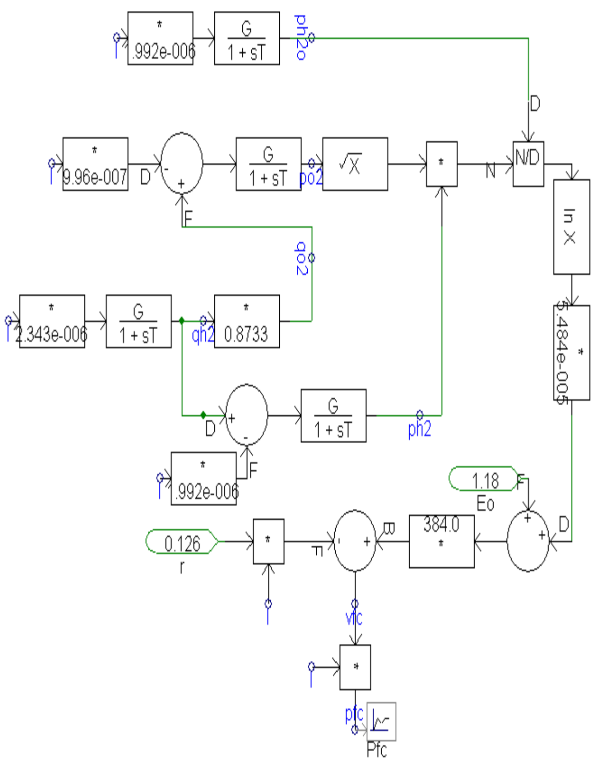

Fig.2 SOFC model in PSCAD/EMTDC

Table 1 Parameters used in SOFC simulation

Representation	Value
Operating temperature (T), K	1273
Faraday's constant (F),C/mol	96487
Universal gas constant (R), J/(kmol K)	8314
Standard reversible cell potential (E), V	1.18
Number of cells (N)	384
Constant (K=$N/4F$), kmol/(s A)	0.996×10^{-6}
Valve molar constant for hydrogen (KH_2), kmol/(s atm)	8.43×10^{-4}
Valve molar constant for oxygen (KO_2), kmol/(s atm)	2.81×10^{-4}
Valve molar constant for water (KH_2O), kmol/(s atm)	2.52×10^{-3}
Response time for hydrogen flow (T_{H2}), sec	26.1
Response time for water flow (T_{H2O}), sec	78.3
Response time for oxygen flow (T_{O2}), sec	2.91
Ohmic loss (r) ,ohm	0.126
Electrical response time (T_e),sec	0.8
Fuel processor response time (T_f) , sec	5
Ratio of hydrogen to oxygen (r_{HO})	1.145

2.2 Photovoltaic model

Solar cells are grouped in larger units to form PV modules, which are then interconnected in a parallel-series configuration to form PV arrays. The output voltage of the solar cell is a function of the photocurrent that depends on the solar irradiation level during its operation. The output current of the solar cell is represented by equation (10). For the PV array consisting of N_s series module and N_p parallel branches, the PV voltage and current are given by equations (11) and (12). The power output of the PV array is the product of output current and output voltage of PV, which is represented by equation (13).

$$I_c = I_{ph} - I_o = I_{ph} - I_{sat}\left[e^{\frac{q}{AKT_c}(V + IR_S)} - 1 \right] \quad (10)$$

$$V_{PV} = N_S \times \left(V_{ref} - \beta\left(T - T_{ref}\right) - R_S\left(T - T_{ref}\right)\right) \quad (11)$$

$$I_{PV} = N_P \times \left(I_{ref} + \alpha\left(\frac{G}{1000}\right)\left(T - T_{ref}\right) + \left(\frac{G}{1000} - 1\right) I_{sc}\right) \quad (12)$$

$$P_{pv} = I_{pv} \times V_{pv} \quad (13)$$

where,

I_{ph} : Light generated current in a solar cell
I_o : Reverse saturation current of diode
T_c : Cell temperature in Kelvin
A : Ideality factor
K : Boltzman constant
q : Electron charge
α : Current temperature coefficient
G : Irradiance
β : Voltage temperature coefficient
N_s : Number of modules connected in series
N_p : Number of modules connected in parallel

2.3 DC/DC Converter model

To connect the DG units to external power system, it is necessary to boost the DG units voltage. To achieve this, a boost or DC/DC converter is used to step-up and to regulate the DG voltage. Figure 3 shows the simulated DC/DC converter model.

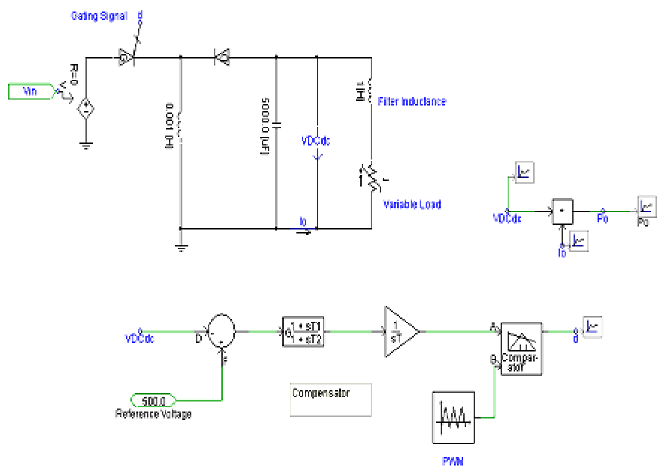

Fig.3 DC/DC Converter model

2.4 DC/AC Converter model

The DC/AC converter or PWM inverter is modeled in PSCAD/EMTDC by using a three-phase voltage source converter averaged model as shown in Figure 4. To reduce harmonics, filters are connected between the converter and the main grid. The first order filter is represented by the inductance, L and resistance, R. In Figure 4, E_{grida}, E_{gridb} and E_{gridc} are the three-phase AC output voltagea of the inverter and I_a,I_b and I_c are the three-phase AC output currents of the inverter.

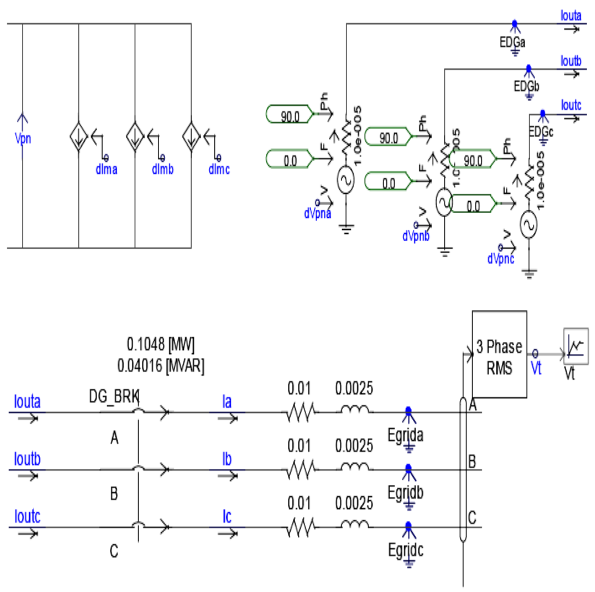

Fig.4 Three-phase DC/AC converter

3 Proposed Inverter Control Strategy

Two DG units are considered in this study in which the interconnection between the two DG units with the main grid at the point of common coupling is as shown in Figure 1. Each DG unit comprises of a DC source and a voltage source inverter. The configuration of the VSI used in each DG unit is shown in Figure 5. The inverter transfers energy produced by the DG and at the same time controls the power flow by using impedances with resistance *R1*, inductance *L1* and parallel capacitive filter. These impedances provide a path for some high-order harmonics generated at the switching frequency. For the inverter operating in voltage control mode, its controller generates three reference signals, E_{grida}, E_{gridb}, E_{gridc}, each of which is referred to the output voltage that is to be applied on each phase, so that the currents I_a, I_b, I_c, track its desired values corresponding to the power flows required between the DC and AC sides. The output voltages of the VSI are required to track the reference voltages by applying the pulse width modulation (PWM) technique.

The proposed inverter control strategy is explained in terms of three different modes of operation, namely, i) grid connected mode (Switch close), ii) islanding mode (Switch open) and iii) transition mode (Switch open and close within 2 seconds). When the inverter operates in grid connected mode, it uses both power and current control while in islanding mode, it uses voltage control.

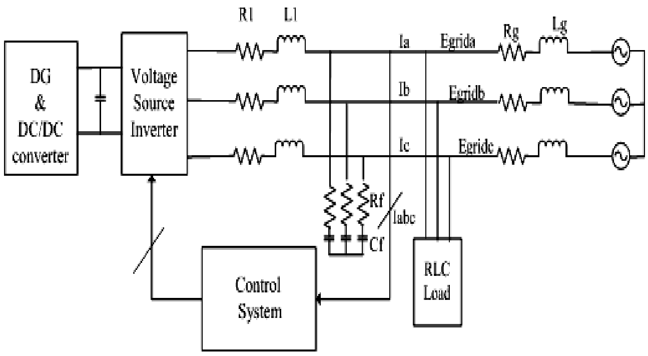

Fig. 5 Inverter control system for each DG

3.1 Control for grid-connected operation

In grid-connected mode of operation, the voltage and frequency are controlled by the grid. Thus, the DG units are controlled to provide specified amount of real power depending to the ratings of the units. Therefore, current control and power control are used in the grid-connected mode of operation as shown in Figure 6. To control the active and reactive output powers, the developed control system is implemented in the *dq0* reference frame. The inverter output current components, *Id* and *Iq* are controlled by means of some current reference values, I_{dref} and I_{qref}, obtained from the outputs of the power control block shown in Figure 5. Power measurement is made at the inverter output and the powers are compared with the power reference values, P_{ref} and Q_{ref}. The difference between the output and the reference powers, *dP* and *dQ*, provides inputs to a PI controller which allows generation of the reference signals, I_{dref} and I_{qref}. A comparison is made to provide the error signals which are subsequently passed through the PI controller to obtain the inverter modulating signals of the PWM. Then, by using the *dq0-to-abc* transformation block, the pulse signals for the inverter are obtained. The PWM implementation of the VSI is also shown in Figure 7.

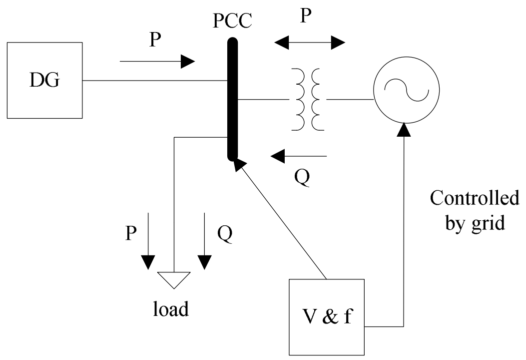

Fig.6 Grid-connected mode of operation

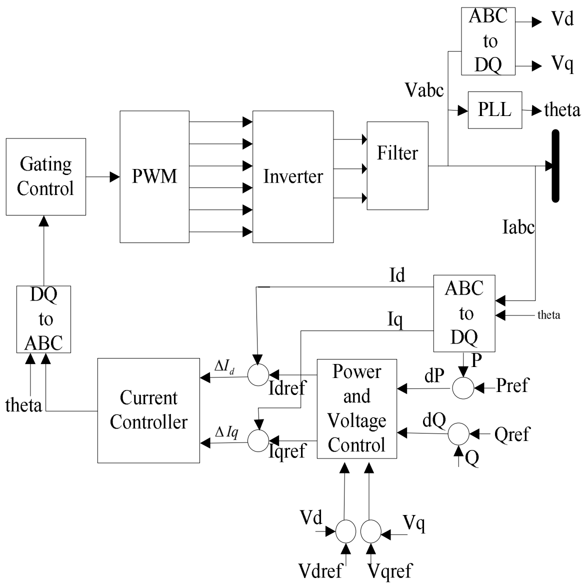

Fig.7 PWM Control of Voltage Source Inverter

3.2 Control for islanding operation

In islanded mode of operation, the frequency and voltage regulation are assigned to the DG unit. When mains supply power is lost due to network faults, the DG units will continue to supply the connected load as shown in Figure 8. In order to accomplish an islanding mode operation for the microgrid system, a suitable control is required for the DG units. Since the system is disconnected from the utility grid in the islanding mode of operation, the voltage is no longer regulated by the grid. Therefore, a control scheme is needed to actively regulate the local voltage. In this control scheme the inverters are operated as voltage control inverters. In the islanding mode, inverter can no longer track the grid voltage and it needs to have an external frequency reference.

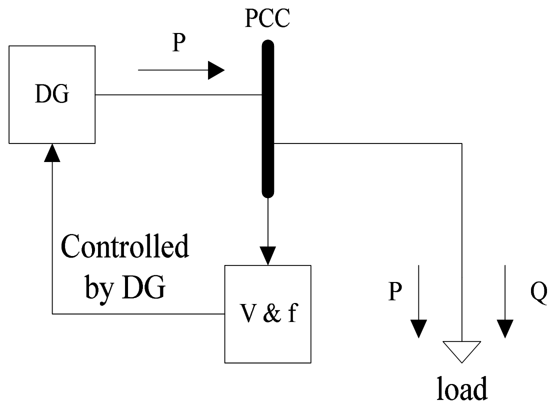

Fig.8 Islanded mode of operation

During the operation of the microgrid system from the islanding mode to the grid-connected mode, the inverter output voltage has to be synchronized to the grid and this can be achieved by using a phase-locked loop (PLL). The PLL assists to track and transform the VSI voltage into angle theta. Special consideration needs to be taken into account for the generation of the angle. Once synchronization is achieved, the grid and VSI voltages are made equal to ensure synchronism.

4 Simulation Results

The performance of the proposed inverter control strategies are evaluated by simulations using the PSCAD/EMTDC simulation software. Simulations were carried out to investigate the effectiveness of the combined power and voltage control scheme in managing power sharing among the DG units in a microgrid. Simulation results are presented for the performance of the DGs in grid connected (Switch close), islanding mode (Switch open) and transition mode (Switch open and close within 2 seconds) of operations.

4.1 Results of DG in grid connected mode of operation

In the simulation for grid connected mode of operation, initially the transfer switch is turned on (Switch close) at 0.2s. The DG inverters are now controlled by using the power control scheme so as to manage power sharing among the DG units. The variation of active power of DGs and loads are shown in Figures 9 and 10, respectively. From Figure 9, the active power from the grid is 0.25MW while the power from both DG units is 0.05MW. Hence, the total power generated is 0.35 MW. Figure 10 shows that load 1, 2 and 3 consume similar power of about 0.100MW, thus giving a total load of 0.3 MW. Voltage profiles for DG and grid are shown in Fig.11.

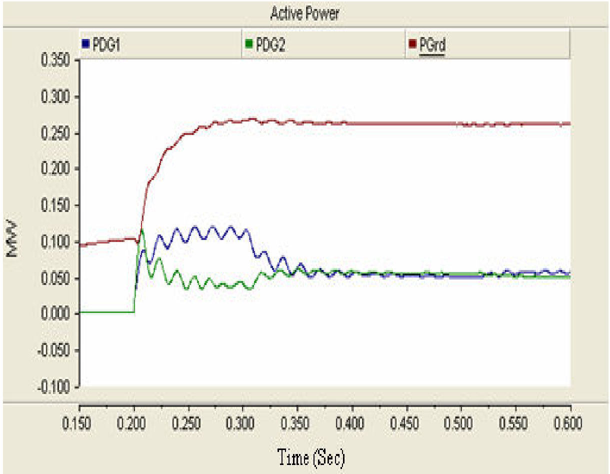

Fig.9 Active power of DGs and grid

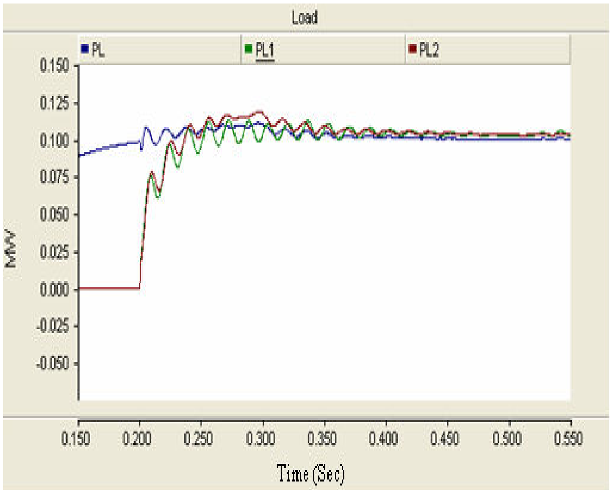

Fig.10 Active power of loads

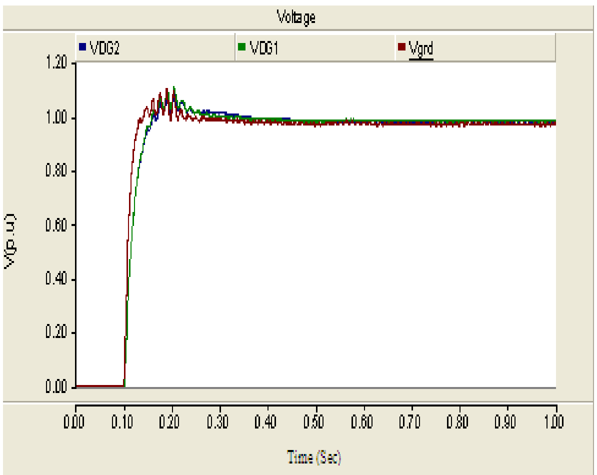

Fig.11 Comparison of voltage profiles at DG1, DG2 and grid

The next simulation results show the effect of increasing all the loads at t= 1s as shown in Figures 12 and 13. From Figure 12, it can be seen that the active power from the grid reduces slightly to 0.23 MW while the power from both DGs increases greatly to 0.5 MW. The increase in power is to provide sufficient power to the loads which is increased to 0.55 MW as shown in Figure 13.

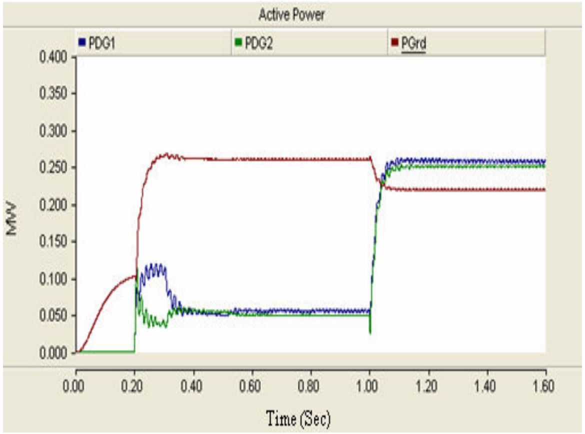

Fig.12 DGs and grid powers during load increase

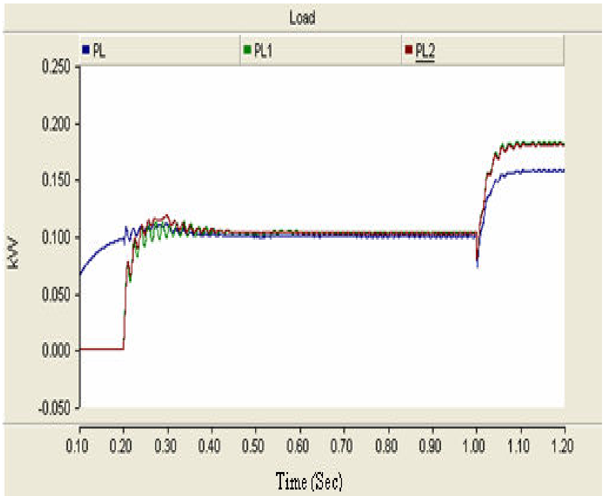

Fig.13 Load powers during load increase

4.2 Results of DG in islanding mode of operation

In the simulation for islanding mode of operation, the transfer switch is turned off (Switch open) at 0.2s. The voltage control scheme of the DG inverters is now activated to allow the DG units to continue supply power to the loads and at the same time to meet the voltage amplitude and frequency reference of the main grid. The variation of active power of DGs and loads in the islanding operation are shown in Figures 14 and 15, respectively. Under this condition, the DG units generate higher power so as to meet the load requirements.

Figure 14 and Figure 15 show the total power generated by the DG units and the total power of load which is approximately 0.3 MW and 0.255 MW, respectively. The voltage profile for both DGs during islanded mode of operation with the static load connected to the DG units is shown in Figure 16.

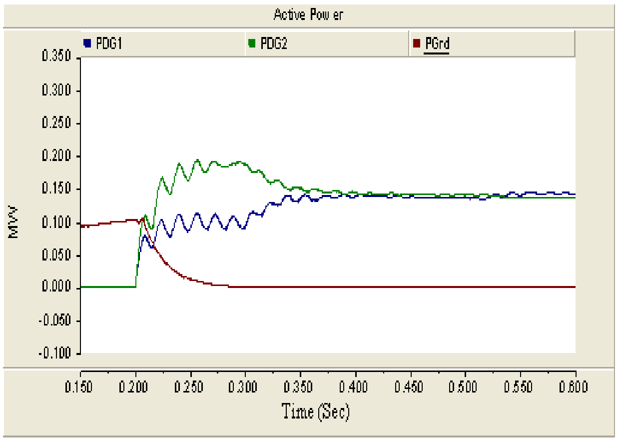

Fig.14 DGs and grid powers during islanding

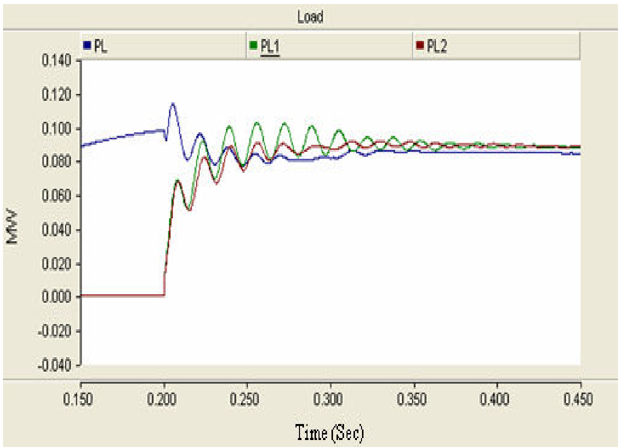

Fig. 15 Load powers during islanding

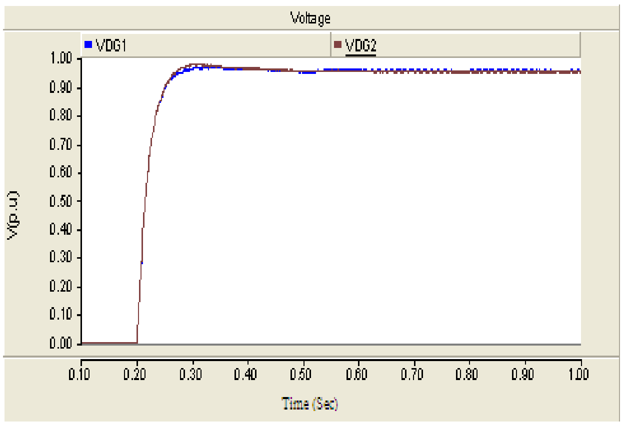

Fig.16 Voltage profile of DG1 and DG2

4.3 Results of DG in transition mode of operation

In the simulation for transition mode of operation, the transfer switch is first turned on (Switch close) and operates in the power control scheme. At 4s later, the transfer switch is turned off (Switch open) so as to disconnect the grid from the system. The DG units increase its power to compensate for the loss of grid supply during 4s to 6s time period as shown in Figure 17. The simulation shows that the proposed method for controlling the DG units is effective during the 2s islanding period. In addition, the voltage control scheme guarantees continuity of power supply to the loads even during islanding from the main utility grid. When this happens, the inverter responds accordingly, with the load voltage returning quickly to its pre-disturbance value as shown in Figure 18.

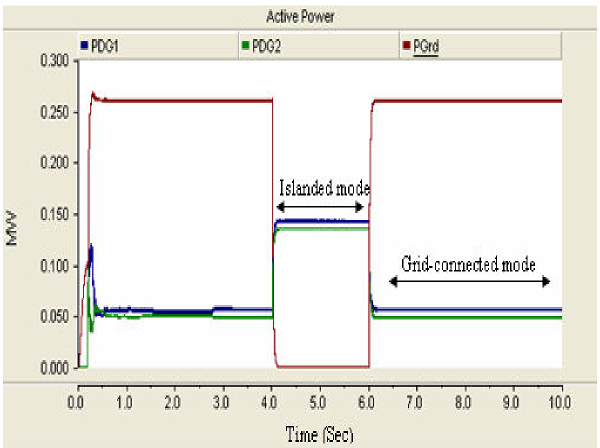

Fig.17 Transition mode with the DG units in operation

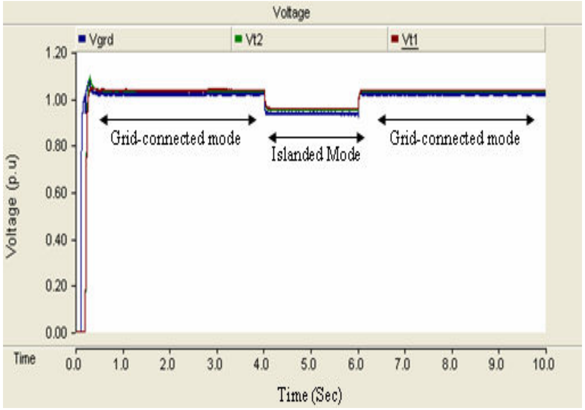

Fig.18 Comparison of voltage profiles at DG1, DG2 and grid

5 Conclusion

Improved control strategy for SOFC and PV inverters used in a microgrid is established in this work. The control strategy is based on combined power control and voltage control schemes to control the SOFC and PV voltage source inverters. The effectiveness of the control strategy is evaluated by operating the microgrid in grid connected, islanding and transition modes of operation. Test results showed that the proposed control strategy is able to correctly manage power sharing among the DG units in a microgrid, regulate quickly the DG power outputs to meet the requirements of the loads, tolerate the rapid changes in various mode of operations and maintain voltage quality at the grid and loads.

References:

[1] R Lasseter, A Akhil, C Marnay, Integration of Distributed Energy Resources, *The CERTS Microgrid Concept*, LBNL-50829, Lawrence Berkeley National Laboratory, 2002

[2] H. H. Zeineldin, E. F. El-Saadany, and M. M. A. Salama, Impact of DG Interface Control on Islanding Detection and Non-detection zones, *IEEE Transactions on Power Delivery*, Vol. 21, No. 3, 2006, pp. 1515-1523.

[3] K. Sung-Hun, S. R. Lee, H. Dehbonei et al., Application of Voltage and Current-controlled Voltage Source Inverters for Distributed Generation Systems, *IEEE Transaction on Energy Conversion*, Vol. 21, No. 3, 2006, pp. 782-792.

[4] G. Fang, and M. R. Iravani, A Control Strategy for a Distributed Generation Unit in Grid-Connected and Autonomous Modes of Operation, *IEEE Transactions on Power Delivery*, Vol. 23, No. 2, pp.850-859, 2008

[5] T C Green and M. Prodanovic, Control of Inverter-based Microgrids, *Electric Power Systems Research*, Vol.77, Issue 9, 2007, pp.1204-1213.

[6] F Katiraei, M R Iravani, P W Lehn, Micro-Grid Autonomous Operation During and Subsequent to Islanding Process, *IEEE Trans. on Power Delivery*, Vol.20, No.1, 2005, pp.248-257.

[7] J. A. Peças Lopes, C. L. Moreira, and A. G. Madureira, Defining Control Strategies for MicroGrids Islanded Operation, *IEEE Transactions on Power System*, Vol 21, Issue 2, 2006, 916 -924.

[8] S K Chung, Phase-locked Loop for Grid-Connected Three-phase Power Conversion Systems, *Proc. Inst. Elect. Eng*, Vol. 147, No. 3, 2000, pp. 213–219.

[9] K De Brabandere, B Bolsens, J Van den Keybus, A. Woyte, J. Driesen, and R. Belmans, A Voltage and Frequency Droop Control Method for Parallel Inverters, *IEEE Transactions on Power Electronics*, Vol.22, No.4, 2007, pp.1107-1115.

[10] Y Zhu, K Tomsovic, Development of Models for Analyzing the Load Performance of Microturbines and Fuel Cells, *Electric Power System Research* 62, 2002, pp.1-11.

[11] A A Salam, M A Hannan, A Mohamed, Dynamic Modeling and Simulation of Solid Oxide Fuel Cell System,*2nd IEEE International Conference on Power and Energy* PECON 2008, 1-3 December 2008, Johor Bahru, MALAYSIA.

[12] S Moulahoum, O Touhami, A Rezzoug, L.Baghli, Rectified Self-Excited Induction Generator as Regulated DC Power Supply for Hybrid Renewable Energy Systems, *WSEAS Transactions on Circuits and Systems,* Vol.4, Issue 11, Nov. 2005, pp. 1457-1464.

[13] A Kuperman, R Rabiniovici, Shunt Voltage Regulators for Autonomous Induction Generators, Part 1: Principles of Operation, *WSEAS Transactions on Power Systems,* Vol.1, Issue 1, Jan. 2006, pp. 221-226

[14] A Kuperman, R Rabiniovici, Shunt Voltage Regulators for Autonomous Induction Generators, Part 2: Circuits and Systems, *WSEAS Transactions on Power Systems,* Vol.1, Issue 1, Jan. 2006, pp.227-232.

[15] D. Ardito, S. Conti, S. Raiti, U. Vagliasindi, Storage Systems Reliability in Stand-Alone PV Applications: RFC&URFC,*WSEAS Transactions*

on Power Systems, Vol. 1, No. 2, February 2006, pp. 358 - 365
[16]Golkar M.A, Distributed Generation an Overview, *The Sixth WSEAS International Conference on Power Systems*, September 22-24, 2006, Lisbon, Portugal